Flow of a thin liquid film on an unsteady stretching sheet

B. S. Dandapat[a] and S. Maity
Physics and Applied Mathematics Unit, Indian Statistical Institute, 203, B. T. Road, Calcutta-700 108, India

(Received 5 December 2005; accepted 12 September 2006; published online 16 October 2006)

The stretching surface is assumed to be stretched impulsively from rest and the effect of inertia of the liquid is considered. Equations describing the laminar flow on the stretching surface are solved analytically by using the singular perturbation technique and the method of characteristics is used to obtain an analytic expression for film thickness. The results show that the final film thickness is independent of the amount of liquid distributed initially and on the initial film thickness be it uniform or nonuniform. It is also shown that the forceful stretching produces quicker thinning of the film on the stretching surface. [DOI: 10.1063/1.2360256]

I. INTRODUCTION

The flow of thin liquid film is important for the understanding and design of various heat exchangers and chemical processing equipment. Applications include wire and fiber coating, polymer processing, etc. In a melt-spinning process, the extrudate from the die is generally drawn and simultaneously stretched into a filament or sheet, which is then solidified through rapid quenching or gradual cooling by direct contact with water or chilled metal rolls. In fact, stretching imparts a unidirectional orientation to the extrudate, thereby improving its mechanical properties and the quality of the final product. A crude model of a class of flow problems with obvious relevance to polymer extrusion is the flow, induced by the stretching motion of a flat elastic sheet as depicted in Fig. 1. Polymer melt from the chamber A is spilled over an elastic sheet through a slit B. This spilled-over polymer starts flowing when the elastic sheet is stretched along its plane. It is obvious, that a boundary layer is developed near the slit B, but this boundary layer will soon grow and cover the entire fluid blob at a short downstream distance C. To study this flow configuration, Crane[1] first modelled this flow configuration as a steady two-dimensional boundary layer flow caused by the stretching of a flat sheet which moves in its own plane with velocity varying linearly with distance from a fixed point and gave an exact similarity solution in closed analytical form. It is understandable that the solution provided by Crane is valid in between the region B to C. Due to its practical applications, the stretching sheet problem has attracted several researchers for the last three decades and is extensively studied to understand the same, along with either the sole effects of rotation, heat and mass transfer, chemical reaction, MHD, suction/injection, non-Newtonian fluid or different possible combinations of these above effects.[2–18] Needless to say that in all these studies, the boundary layer equation is considered and the boundary conditions are prescribed at the sheet and on the fluid outside the boundary layer (at infinity). Imposition of similarity transformation reduces the system to a set of ODEs, which are then solved either analytically or numerically. Wang[19] first studied the unsteady boundary layer flow of a finite liquid film. In this study, he restricted the motion to a specified family of time dependence and reduced the boundary layer equations to a nonlinear ODE involving a nondimensional unsteady parameter by using a special type of similarity transformation. Using this special type of similarity transformation, Andersson *et al.*[20] have studied the unsteady stretching flow in the case of power-law fluid film. Later on Andersson *et al.*[21] and Dandapat *et al.*[22] extended Wang's unsteady thin film stretching problem to the case of heat transfer and Chen[23] explored the heat transfer in a power-law fluid. To the best of our knowledge, we like to state here that the study of unsteady flow due to stretching of a sheet has not yet received adequate attention when the film and the boundary layer thickness coincide despite the extensive research made on this flow problem since the last three decades.

If the thickness of liquid film either coincides or lies within the boundary layer thickness, then one needs to consider full momentum equations to study such flow problem. Based on this principle, we have considered the full Navier-Stokes equations and the equation of continuity to study the thin liquid film flow due to the stretching sheet under following assumptions:

(i) The initial film thickness $h=h(x,t)$ is known at the onset of stretching, i.e., at time $t=0$.
(ii) Once the stretching starts, no fluid enters into the system. Only the existing fluid over the sheet flows along the stretching direction and hence the film thickness changes continuously along that direction.
(iii) The elastic sheet is much larger than the film thickness, so that no further liquid spills from the elastic sheet.
(iv) Adjacent to the liquid film at the free surface is a gas or liquid vapor, and therefore the viscosity ratio, μ_g/μ_l (where μ_l and μ_g are the viscosity of the liquid and gas phase, respectively) is much less than unity and any motion of the gas is neglected.

The paper is organized as follows: Mathematical formulation for the problem is presented in Sec. II. Section III contains

[a]Author to whom correspondence should be addressed. Electronic mail: dandapat@isical.ac.in

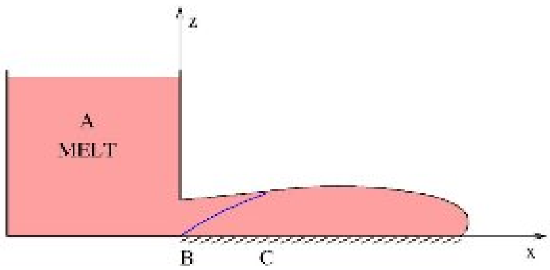

FIG. 1. Schematic flow diagram.

the derivation of the evolution equation and its solution. Results and discussions are given in Sec. IV and finally, Sec. V is devoted to the conclusion.

II. MATHEMATICAL FORMULATION

Let the x axis be chosen along the plane of the stretching sheet and the z axis is taken to be normal to the plane. We assume that the surface at $z=0$ starts stretching impulsively from rest with stretching rate xf_0, f_0 being constant with the dimension of $[\text{time}]^{-1}$. Due to impulsive stretching, the viscous force causes the fluid to move along its own plane. At the initial stage, this motion is imparted from the plane to the adjacent fluid layer and then gradually spreads out to the entire depth of the film by viscosity. As time increases, the fluid continues to flow in the outward direction and the thickness of the film gradually decreases resulting in an increase of viscous resistance so as to balance the impulsive inertial force. At this stage the Reynolds number $\text{Re}(\equiv u_0 h_0/\nu)$ is of $O(1)$ and balance of aforesaid forces defines a characteristic time scale $t_c=\nu/h_0^2 f_0^2$, where h_0 and ν denote the initial film thickness of the liquid film and kinematic viscosity of the fluid, respectively, u_0 denotes the characteristic velocity defined as L/t_c, where L is the characteristic length scale along the stretching direction. The nondimensional equations of motion and the equation of continuity are obtained by using the following nondimensional variables:

$$\hat{x}=\frac{x}{L}, \quad \hat{z}=\frac{z}{h_0}, \quad \hat{h}=\frac{h}{h_0}, \quad \hat{t}=\frac{t}{t_c}, \quad \hat{u}=\frac{u}{u_0},$$
$$\hat{w}=\frac{w}{\epsilon u_0}, \quad \hat{p}=\frac{p h_0^2 t_c}{\rho \nu L^2}, \tag{1}$$

in dimensional governing equations and finally by dropping the hat over the variables, we obtain

$$\epsilon\,\text{Re}\left[\frac{\partial u}{\partial t}+u\frac{\partial u}{\partial x}+w\frac{\partial u}{\partial z}\right]=-\frac{\partial p}{\partial x}+\epsilon^2\frac{\partial^2 u}{\partial x^2}+\frac{\partial^2 u}{\partial z^2}, \tag{2}$$

$$\epsilon^3\,\text{Re}\left[\frac{\partial w}{\partial t}+u\frac{\partial w}{\partial x}+w\frac{\partial w}{\partial z}\right]=-\frac{\partial p}{\partial z}+\epsilon^4\frac{\partial^2 w}{\partial x^2}+\epsilon^2\frac{\partial^2 w}{\partial z^2} - \epsilon F^{-2}\,\text{Re}, \tag{3}$$

$$\frac{\partial u}{\partial x}+\frac{\partial w}{\partial z}=0. \tag{4}$$

Here ϵ is a dimensionless parameter defined as h_0/L which is assumed to be small and $F=\sqrt{u_0^2/gh_0}$ is the Froude number.

Following are the corresponding boundary and initial conditions in dimensionless form:

- *No-slip condition on the plane $z=0$:*

$$u(t,x,0)=ax, \quad w(t,x,0)=0, \tag{5}$$

where $a=f_0 t_c$ is the measure of the impulsive stretching strength.

- *Jump in the normal stress across the interface is balanced by the surface tension times curvature at $z=h(x,t)$:*

$$-p+2\epsilon^2\left[\epsilon^2\frac{\partial h}{\partial x}\left(\frac{\partial u}{\partial x}\frac{\partial h}{\partial x}-\frac{\partial w}{\partial x}\right)+\left(\frac{\partial w}{\partial z}-\frac{\partial u}{\partial z}\frac{\partial h}{\partial x}\right)\right]\times\left\{1+\epsilon^2\left(\frac{\partial h}{\partial x}\right)^2\right\}^{-1} = \epsilon^3\,\text{We}\,.\,\text{Re}\,\frac{\partial^2 h}{\partial x^2}\left\{1+\epsilon^2\left(\frac{\partial h}{\partial x}\right)^2\right\}^{-3/2}, \tag{6}$$

where $\text{We}=\sigma/\rho h_0 u_0^2$ is the Weber number and ρ denotes the density of the fluid.

- *Shear stress vanishes along the interface $z=h(x,t)$:*

$$2\epsilon^2\frac{\partial h}{\partial x}\left[\frac{\partial w}{\partial z}-\frac{\partial u}{\partial x}\right]+\left[\frac{\partial u}{\partial z}+\epsilon^2\frac{\partial w}{\partial x}\right]\left\{1-\epsilon^2\left(\frac{\partial h}{\partial x}\right)^2\right\}=0. \tag{7}$$

- *The kinematic condition at $z=h(x,t)$:*

$$\frac{\partial h}{\partial t}+u\frac{\partial h}{\partial x}=w. \tag{8}$$

- *The initial conditions at $t=0$:*

$$u(0,x,z)=w(0,x,z)=0,$$
$$h(0,x)=\delta(x). \tag{9}$$

III. ASYMPTOTIC ANALYSIS

To solve the system of nonlinear partial differential equations (2)–(9), we expand the dependent variables in power of ϵ as

$$F(x,z,t)=\sum \epsilon^j F_j(x,z,t). \tag{10}$$

Substituting (10) into the system of equations (2)–(9) and equating different powers of ϵ we can obtain sets of equation involving variables u, w, and p. Solving for u, w, and p up to first order, we get

$$u=ax+\epsilon\,\text{Re}[a^2x+F^{-2}h_x-\epsilon^2\,\text{We}\,h_{xxx}]\left(\frac{z^2}{2}-hz\right),$$

$$w=-az+\epsilon\,\text{Re}\left[(a^2+F^{-2}h_{xx}-\epsilon^2\,\text{We}\,h_{xxxx})\left(-\frac{z^3}{6}+\frac{hz^2}{2}\right)+(a^2x+F^{-2}h_x-\epsilon^2\,\text{We}\,h_{xxx})\left(\frac{z^2h_x}{2}\right)\right], \tag{11}$$

$$p = \epsilon \mathrm{Re}[F^{-2}(h - z) - \epsilon^2 \mathrm{We}\, h_{xx}],$$

where h_x denotes $\partial h/\partial x$. It is clear from Eq. (11) that these solutions do not satisfy the initial condition (9). This is due to the fact that, our characteristic time t_c is large. To obtain the initial developments we need to stretch the time coordinate to achieve the small time solution and then match both solutions by the composite matching principle (Van Dyke[24]). Substituting (11) into (8), we get

$$\frac{\partial h}{\partial t} = \frac{\partial}{\partial x}\left[- axh + \frac{\epsilon \mathrm{Re}}{3}\{a^2 x + F^{-2} h_x - \epsilon^2 \mathrm{We}\, h_{xxx}\} h^3 \right]. \tag{12}$$

To solve (12), we expand h as in Eq. (10) and collect the coefficients of order up to ϵ, and obtain at the lowest order the following governing equation:

$$h_{0t} + axh_{0x} = - ah_0 \tag{13}$$

while at the order ϵ, we have

$$h_{1t} + axh_{1x} = - ah_1 + \mathrm{Re}\left[\{a^2 x + F^{-2} h_{0x} - \epsilon^2 \mathrm{We}\, h_{0xxx}\} \frac{h_0^3}{3} \right]_x. \tag{14}$$

It follows from Eq. (13) that

$$\frac{d}{dt} h_0(x(t),t) = - ah_0(x(t),t), \tag{15}$$

along the characteristic curve $x(t)$ satisfying

$$\frac{dx(t)}{dt} = ax(t). \tag{16}$$

Upon integration, these two equations give

$$h_0 = C_0 e^{-at} \quad \text{along} \quad x = C_1 e^{at}. \tag{17}$$

It follows from (17) that along each characteristic curve (16)

$$xh_0 = C_0 C_1 = \text{constant}. \tag{18}$$

Here, C_0 and C_1 are characteristic-curve dependent constants. Since the above equations are valid at large times, these constants C_0 and C_1 can be related to the initial data by matching these solutions with small time solutions which we discuss in Sec. III. Similarly, following the same principle, we can integrate (14) along the same characteristic curve (16) to obtain h_1 as

$$h_1 = \mathrm{Re}\left[\frac{a}{3} e^{-3at} - \frac{F^{-2} C_0 C_1^{-2}}{3a} e^{-6at} + \frac{2\epsilon^2 \mathrm{We}\, C_0 C_1^{-4}}{a} e^{-8at} \right] C_0^3 + C_2 e^{-at}, \tag{19}$$

along the characteristic curve (16). In Eq. (19), C_2 is the integration constant. In order to find the values of the constants C_0, C_1, and C_2 we need to match these solutions with short-time solutions.

Short-time analysis: At the viscous diffusion stage, the time scale is dictated by the fact that the local inertial term is of the same order of magnitude as the viscous terms in the governing equations. The appropriate time scale is then given by $\tau = t/\epsilon$ and we keep other independent variables as these are, only the dependent variables are denoted with over bar. The corresponding nondimensional equations for momentum, continuity, boundary, and initial conditions reduce, for the *short time scale* as

$$\mathrm{Re}\frac{\partial \bar{u}}{\partial \tau} + \epsilon\, \mathrm{Re}\left[\bar{u}\frac{\partial \bar{u}}{\partial x} + \bar{w}\frac{\partial \bar{u}}{\partial z} \right] = - \frac{\partial \bar{p}}{\partial x} + \epsilon^2 \frac{\partial^2 \bar{u}}{\partial x^2} + \frac{\partial^2 \bar{u}}{\partial z^2},$$

$$\epsilon^2\, \mathrm{Re}\frac{\partial \bar{w}}{\partial \tau} + \epsilon^3\, \mathrm{Re}\left[\bar{u}\frac{\partial \bar{w}}{\partial x} + \bar{w}\frac{\partial \bar{w}}{\partial z} \right] = - \frac{\partial \bar{p}}{\partial z} + \epsilon^4 \frac{\partial^2 \bar{w}}{\partial x^2} + \epsilon^2 \frac{\partial^2 \bar{w}}{\partial z^2} - \epsilon F^{-2}\, \mathrm{Re},$$

$$\frac{\partial \bar{u}}{\partial x} + \frac{\partial \bar{w}}{\partial z} = 0.$$

The associated boundary conditions reduce to

$$\bar{u}(\tau,x,0) = ax, \quad \bar{w}(\tau,x,0) = 0, \quad \text{at } z = 0;$$

$$\left.\begin{aligned}
&- \bar{p} + 2\epsilon^2 \left[\epsilon^2 \frac{\partial \bar{h}}{\partial x}\left(\frac{\partial \bar{u}}{\partial x}\frac{\partial \bar{h}}{\partial x} - \frac{\partial \bar{w}}{\partial x} \right) + \left(\frac{\partial \bar{w}}{\partial z} - \frac{\partial \bar{u}}{\partial z}\frac{\partial \bar{h}}{\partial x} \right) \right]\left\{ 1 + \epsilon^2 \left(\frac{\partial \bar{h}}{\partial x} \right)^2 \right\}^{-1} = \epsilon^3\, \mathrm{We}\, .\, \mathrm{Re}\frac{\partial^2 \bar{h}}{\partial x^2}\left\{ 1 + \epsilon^2 \left(\frac{\partial \bar{h}}{\partial x} \right)^2 \right\}^{-3/2} \\
&2\epsilon^2 \frac{\partial \bar{h}}{\partial x}\left[\frac{\partial \bar{w}}{\partial z} - \frac{\partial \bar{u}}{\partial x} \right] + \left[\frac{\partial \bar{u}}{\partial z} + \epsilon^2 \frac{\partial \bar{w}}{\partial x} \right]\left\{ 1 - \epsilon^2 \left(\frac{\partial \bar{h}}{\partial x} \right)^2 \right\} = 0 \\
&\frac{\partial \bar{h}}{\partial \tau} + \epsilon \bar{u}\frac{\partial \bar{h}}{\partial x} = \epsilon \bar{w}
\end{aligned}\right\} \text{at } z = \bar{h}(x,\tau),$$

$$\left.\begin{aligned}
&\bar{u}(0,x,z) = \bar{w}(0,x,z) = 0 \\
&\bar{h}(0,x) = \delta(x)
\end{aligned}\right\} \text{at } \tau = 0. \tag{20}$$

Following the above asymptotic procedure by expanding all dependent variables as

$$\bar{F}(x,z,t) = \sum \epsilon^j \bar{F}_j(x,z,t),$$

we get from (20) at the leading order as

$$\bar{h}_0 = \delta(x) \quad \text{for } \tau \geq 0,$$

$$\bar{u}_0 = ax\left[1 - 2\sum_{n>0} \frac{\sin(\lambda_n z/\delta)}{\lambda_n} e^{(-\lambda_n^2 \tau/\mathrm{Re}\ \delta^2)}\right], \tag{21}$$

$$\bar{w}_0 = -az - 2a\frac{\partial}{\partial x}\sum_{n>0}\left[x\delta\left(\frac{\cos(\lambda_n z/\delta) - 1}{\lambda_n^2}\right)e^{(-\lambda_n^2 \tau/\mathrm{Re}\ \delta^2)}\right],$$

$$\bar{p}_0 = 0,$$

where $\lambda_n = (2n-1)\pi/2$ To complete the solution, we need to calculate the first-order correction to the film thickness for short time. From the kinematic condition, Eq. (20), we obtain the first-order correction to $\bar{h}_0(\tau,x)$ as

$$\bar{h}_1 = -a\frac{\partial(x\delta)}{\partial x}\tau - 2a\ \mathrm{Re}\left\{x\delta_x\delta^2\sum_{n=1}^{\infty}\frac{(-1)^{n-1}}{\lambda_n^3}\left(e^{(-\lambda_n^2 \tau/\mathrm{Re}\ \delta^2)} - 1\right) + \frac{\partial}{\partial x}\left[x\delta^3\sum_{n=1}^{\infty}\frac{1}{\lambda_n^4}\left(e^{(-\lambda_n^2 \tau/\mathrm{Re}\ \delta^2)} - 1\right)\right]\right\}, \tag{22}$$

where $\bar{h}_1(0,x)=0$ is used. The matching condition that is derived from the requirement that the flow is continuous from the start of the stretching to all succeeding time suggests

$$\lim_{\tau\to\infty} \bar{h}(\tau) = \lim_{t\to 0} h(t). \tag{23}$$

Using (23) in (17) and following Van Dyke's composite matching principle at the leading order, we get

$$C_1 = x(0) = \xi\ (say), \quad C_0 = h_0(0,\xi) = \delta(\xi). \tag{24}$$

Therefore, to find $h_0(t,x)$, one needs first to solve Eq. (17), which reduces to

$$x(t) = \xi e^{at}, \tag{25}$$

for x and then uses this in Eq. (17) to obtain

$$h_0 = \delta(\xi)e^{-at}. \tag{26}$$

It is to be noted here that $x(t)$ given above in Eq. (25) represents the characteristic line along which the film thickness changes with time. The constant C_2 in Eq. (19), can also be estimated by using the matching relation (23) in (19) and (22); this gives

$$C_2 = \mathrm{Re}\left[\frac{3}{2}a\xi\delta_\xi\delta^2 + \frac{1}{3a}F^{-2}\delta^4\xi^{-2} - \frac{2}{a}\epsilon^2\ \mathrm{We}\ \delta^4\xi^{-4}\right]. \tag{27}$$

The composite uniform solution that possesses both the time scales is obtained as

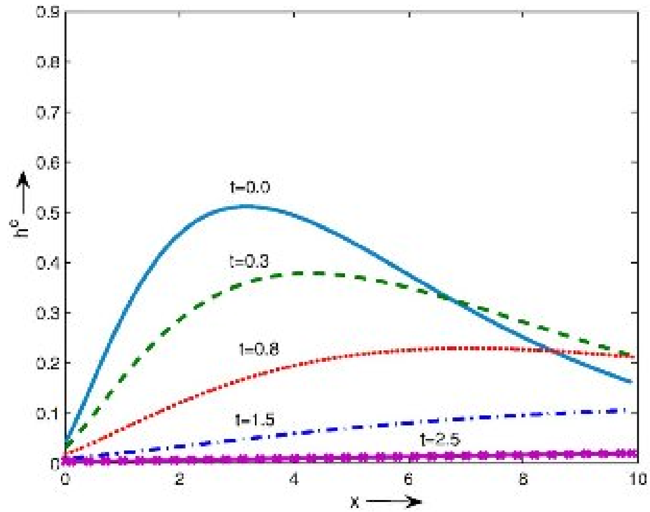

FIG. 2. Variation composite film thickness h^c with respect to x for different values of t when Re=0.21187, F=0.24382, We=0.13921, ϵ=0.001, a=1, and $\delta=0.47(\xi+0.3)^2 \exp^{-\xi^{0.76}}$.

$$h^c = (h_0 + \bar{h}_0 - \delta) - at(\xi\delta)_\xi + \epsilon\,\mathrm{Re}\left[h_1 + \bar{h}_1 - \left(\frac{\delta^3}{3} + \frac{3}{2}\xi\delta_\xi\delta^2\right)\right]. \tag{28}$$

IV. RESULTS AND DISCUSSIONS

By a simple observation of Eq. (21) for $\overline{u_0}$ and $\overline{w_0}$ will reveal that this short time solution reduces to the leading order solution for u and w given in (11) for $\tau\to\infty$. One may also think, for a very small time, the fluid near the free surface is at rest, so that the present solution obtained through short-time analysis should be the same as that of the 2D unsteady boundary layer flow without free surface caused by an impulsively stretched sheet. In this connection it is to be remembered that the underlying assumption in Sec. III, is that the effect of viscosity is felt across the entire film thickness. In other words, there is no region where the inviscid layer is present over the film. As a result, one cannot compare the present result to a 2D boundary layer solution caused by an impulsively stretched sheet. Further large time solution (11) for u depends on x linearly up to the first order term but does not depend on z at the leading order. Both Froude and Weber number appear in Eqs. (11) and (12) at the ϵ order only indicating their effects are small on flow field as well as on film thickness. The short time solution of the film thickness $\bar{h}$ given in (21) and (22) show that the inertial effect resists film thinning due to stretching as the terms proportional to $(e^{-\lambda_n^2 t/\epsilon \mathrm{Re}} - 1)$ are vary small at the beginning. Figure 2 represents the variation of h^c with x at several time steps for nonuniform distribution $\delta=0.47(\xi+0.3)^2 \exp^{-\xi^{0.76}}$, keeping the parameters a=1.0, Re=0.21187, F=0.24382, We=0.13921, and ϵ=0.001 fixed. It is clear from the figure that the film height becomes smooth at time more than t=2.5. This indicates that the initial nonuniform film distribution reduces to a smooth distribution at large time. Further

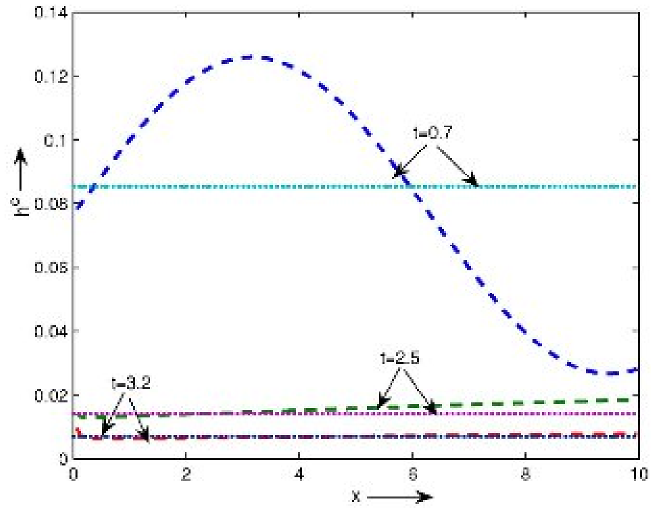

FIG. 3. Comparison of composite film thickness h^c for uniform and nonuniform initial film distribution, where t is fixed when Re=0.21187, F=0.24382, We=0.13921, ϵ=0.001, a=1. Dotted lines are for δ=0.171891 and dashed lines are for δ=0.1535+0.1 sin(ξ).

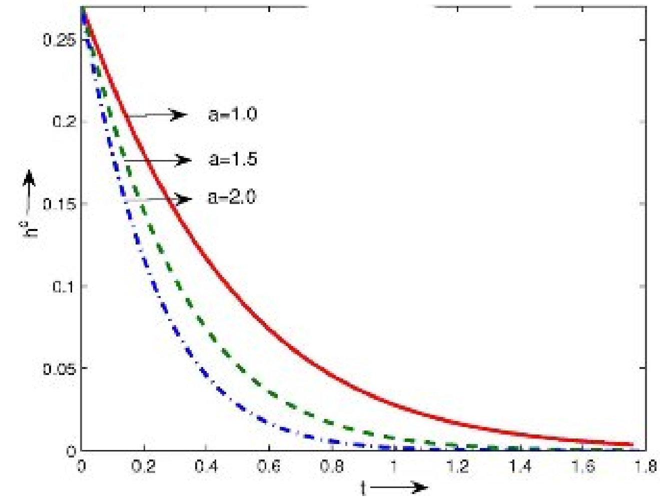

FIG. 4. Variation of composite film thickness h^c with respect to t for different values of a at fixed x=1.5, when Re=0.21187, F=0.24382, We =0.13921, ϵ=0.001 and $\delta=0.47\xi^2 \exp^{-\xi^{0.76}}$.

it is clear from the graph that at time t=2.5 the film thins more in the region $x<1$. A careful scrutiny of Eqs. (19) and (27) give

$$h_1 = \mathrm{Re}\left[a\delta^2\left(\frac{\delta}{3}e^{-3at} + \frac{3}{2}\xi\delta_\xi e^{-at}\right) + \frac{F^{-2}\delta^4\xi^{-2}}{3a}(e^{-at} - e^{-6at}) + \frac{2\epsilon^2\,\mathrm{We}\,\delta^4\xi^{-4}}{a}(e^{-8at} - e^{-at})\right]. \tag{29}$$

This shows that the term containing We is only a negative term which is responsible for tapering of film thickness in the region for $x<1$. In this context we like to point out that earlier we have seen in connection with spin-coating (Emslie *et al.*[25] and Dandapat *et al.*[26]) that all initial irregularities are smoothed out in the course of time and tapering also takes place at the central region of the disk. We have examined several different initial nonuniform distributions and see that the final film thickness becomes smooth at large time. These figures are dropped here to reduce the page length of the manuscript. This above conjecture is further examined in Fig. 3, which depicts h^c versus x at different time t for two sets of initial distributions with the same amount of liquid in both viz. δ_1=0.171891 and δ_2=0.1535+0.1 sin(ξ) are the uniform and nonuniform distributions, respectively. These two distributions are then plotted in Fig. 3 as dotted and dashed lines, respectively, at different time steps. It is evident from the figure that both distributions converge at the same thickness at large time. Based on these observations we can conclude that the final film thickness is insensitive to (a) the amount of liquid distributed initially and (b) the initial film thickness be it uniform or nonuniform. We like to point out here that Eq. (28) is computed along the characteristic lines given in (25). It is clear that the fluid at the point x=0 moves along the characteristic lines as time t increases. According to our assumption (ii), we do not allow the fluid to enter into the system, as a result the point x=0 is shifted to the points $x>0$ as time increases. To avoid the complexity of shifting our computation starts from very near to zero but not from zero. Figure 4 represents the variation of h^c with time t at x=1.5 for different values of a and keeping other parameters fixed. It is clear from the graph that the increased impulsive stretching produces quicker thinning of the film at small time but the film thickness converges to an asymptotic limiting thickness at large time. Figure 5 depicts the variation of u versus z at different time level for fixed x, a, Re, and ϵ for δ=1+0.1 sin(ξ). It is evident from the graph that as time increases, u increases gradually to attain its stretching value at large time. Further the graph manifests that at a fixed small time, u is maximum at the plane of stretching and it decreases as film height increases. But as time increases, the fluid velocity at the free surface also increases rapidly and ultimately at a sufficient time the entire film velocity will be the same. It is also clear from the figure that the film height also decreases as time increases. This trend we have noted

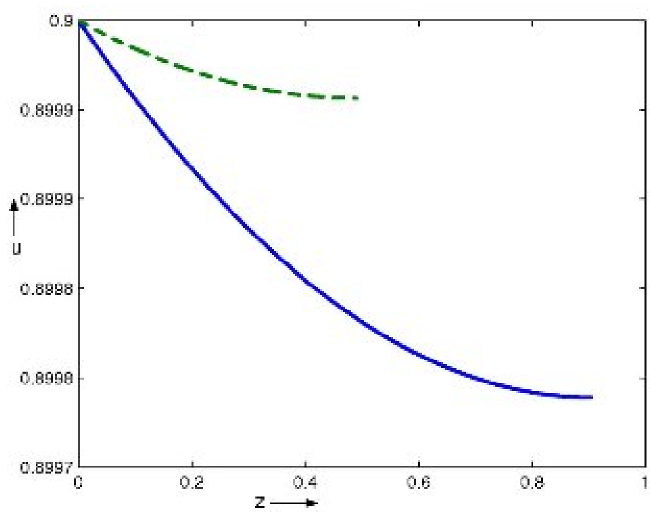

FIG. 5. Variation of velocity u with respect to z at different values of t for Re=0.21187, F=0.24382, We=0.13921, a=1.5, x=0.6, ϵ=0.001, and δ=1+0.1 sin(ξ). Continuous lines are for t=0.1, dotted lines are for t=0.5.

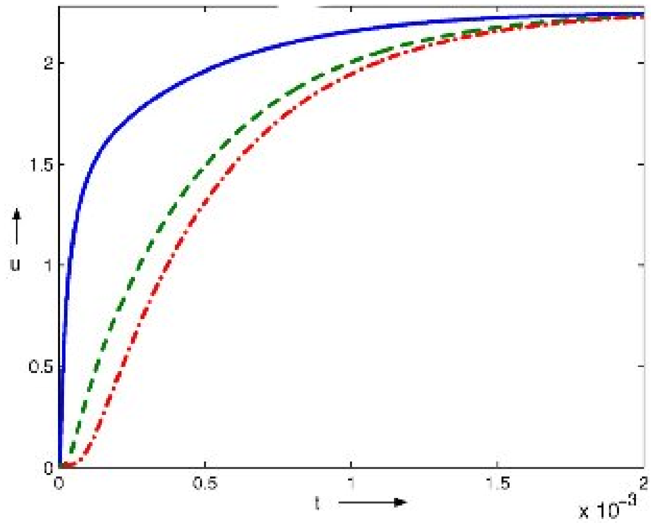

FIG. 6. Variation of velocity u with respect to t for Re=0.21187, $F=0.24382$, We=0.13921, $\epsilon=0.001$, $a=1.5$, $x=1.5$, and $\delta=2+0.3\sin(\xi)$. Continuous lines are for $z=0.2h^c$, dashed lines are for $z=0.6h^c$, and dashed-dotted lines are for $z=h^c$.

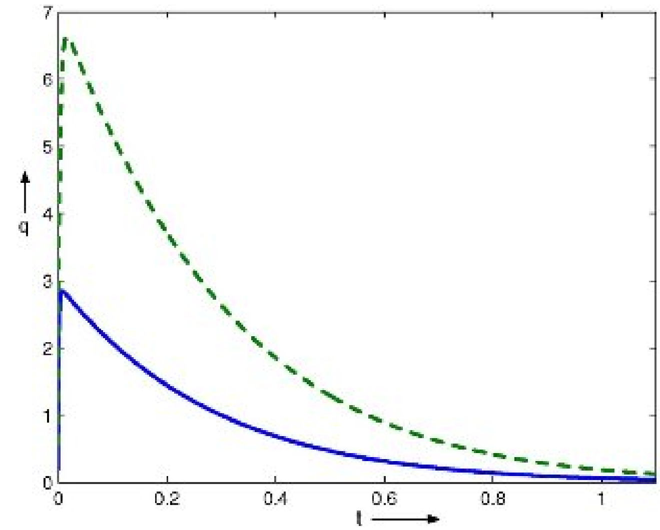

FIG. 8. Variation of flow rate q with respect to t for Re=0.21187, $F=0.24382$, We=0.13921, $\epsilon=0.005$, $a=1.5$, and $\delta=5.2\xi^2\exp^{-\xi^{0.76}}$. Continuous lines are for $x=1$, dashed lines are for $x=1.5$.

earlier. Figure 6 describes the variation of u with time at different heights of the film for the same initial distribution and it confirms the observations made earlier. Figure 7 depicts the variation of w with time at different heights of the film when other parameters Re, a, x, and ϵ are fixed and for the same distribution. Figure 8 shows the variation of flow rate q with time t at different positions along the stretching direction. It is clear from the graph that at the initial stage, the maximum amount of liquid flows out of a particular x along the stretching direction. Further it is evident that the amount of liquid flow gradually decreases with time and ultimately converges to the same amount asymptotically at large time.

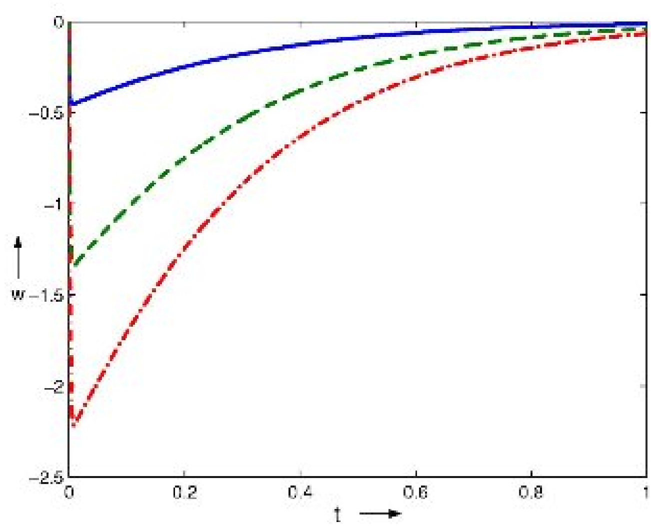

FIG. 7. Variation of velocity w with respect to t for Re=0.21187, $F=0.24382$, We=0.13921, $\epsilon=0.005$, $a=1.5$, $x=1.5$, and $\delta=2.69\xi^2\exp^{-\xi^{0.76}}$. Continuous lines are for $z=0.2h^c$, dashed lines are for $z=0.6h^c$, and dashed-dotted lines are for $z=h^c$.

V. CONCLUSION

We have studied two-dimensional flow of thin liquid film over an impulsively stretching sheet. When the boundary layer thickness coincides with that of the film, boundary-layer equations are no longer valid approximations to study this type of flow problem. Full momentum equations are necessary to solve this flow situation. We have solved the full momentum equations analytically by using the singular perturbation technique and the method of characteristics to obtain an analytic expression for film thickness. In the solution process, we have assumed that the film thickness $h=h(x,t)$ is known at the onset of stretching. It is shown that this initial nonuniform film thickness distribution becomes uniform as time increases. It is also found that the initial film distribution has no effect on the final film thickness at large time. Further, it is found that the initial stretching impulse also has no effect on the final film thickness.

ACKNOWLEDGMENTS

We express our sincere thanks to Professor A. S. Gupta, Professor B. N. Mandal, and Professor H. I. Andersson for critical discussions to carry out this research and the referees for their constructive suggestions and critical comments to improve the text of this paper. S.M. expresses his thanks to CSIR, New Delhi for granting a scholarship to carry out this piece of research.

[1]L. J. Crane, "Flow past a stretching plane," Z. Angew. Math. Phys. **21**, 645 (1970).
[2]C. Y. Wang, "Fluid flow due to a stretching cylinder," Phys. Fluids **31**, 466 (1988).
[3]C. Y. Wang, "The three-dimensional flow due to a stretching surface," Phys. Fluids **27**, 1915 (1984).
[4]C. Y. Wang, "Stretching a surface in a rotating fluid," ZAMP **39**, 177 (1988).
[5]P. S. Gupta and A. S. Gupta, "Heat and mass transfer on a stretching sheet with suction or blowing," Can. J. Chem. **55**, 744 (1977).

[6]L. G. Grubka and K. M. Bobba, "Heat transfer characteristics of a continuous stretching surface with variable temperature," J. Heat Transfer **107**, 248 (1985).
[7]B. K. Dutta and A. S. Gupta, "Cooling of a stretching sheet in a viscous flow," Ind. Eng. Chem. Res. **26**, 333 (1987).
[8]H. I. Andersson, O. R. Hansen and B. Holmedal, "Diffusion of a chemically reactive species from a stretching sheet," Int. J. Heat Mass Transfer **37**, 659 (1994).
[9]R. Kandasamy, K. Periasamy and K. K. S. Prabhu, "Chemical reaction, heat and mass transfer on MHD flow over a vertical stretching surface with heat source and thermal stratification effects," Int. J. Heat Mass Transfer **48**, 4557 (2005).
[10]K. B. Pavlov, "Magnetohydrodynamic flow of an incompressible viscous fluid caused by deformation of a plane surface," Magnetohydrodynamics **4**, 146 (1974).
[11]E. Magyari and B. Keller, "Exact solutions for self-similar boundary-layer flows induced by permeable stretching walls," Eur. J. Mech. B/Fluids **19**, 109 (2000).
[12]H. I. Andersson and B. S. Dandapat, "Flow of a power-law fluid over a stretching sheet," Stability Appl. Anal. Cont. Media **1**, 339 (1991).
[13]A. Chakrabarti and A. S. Gupta, "Hydromagnetic flow and heat transfer over a stretching sheet," Q. Appl. Math. **37**, 73 (1979).
[14]B. S. Dandapat and A. S. Gupta, "Flow and heat transfer in a viscoelastic fluid over a stretching sheet," Int. J. Non-Linear Mech. **24**, 215 (1989).
[15]K. V. Prasad, S. Abel, and P. S. Datti, "Diffusion of chemically reactive species of a non-Newtonian fluid immersed in a porous medium over a stretching sheet," Int. J. Non-Linear Mech. **38**, 651 (2003).
[16]H. I. Andersson, K. H. Bech, and B. S. Dandapat, "Magnetohydrodynamic flow of a power-law fluid over a stretching sheet," Int. J. Non-Linear Mech. **27**, 929 (1992).
[17]B. S. Dandapat, S. N. Singh, and R. P. Singh, "Heat transfer due to permeable stretching wall in presence of transverse magnetic field," Arch. Mech. **56**, 87 (2004).
[18]H. S. Takhar, A. J. Chamkha, and G. Nath, "Flow and mass transfer on a stretching sheet with a magnetic field and chemically reactive species," Int. J. Eng. Sci. **38**, 1303 (2000).
[19]C. Y. Wang, "Liquid film on an unsteady stretching surface," Q. Appl. Math. **48**, 601 (1990).
[20]H. I. Andersson, J. B. Aarseth, N. Braud, and B. S. Dandapat, "Flow of a power-law fluid on an unsteady stretching surface," J. Non-Newtonian Fluid Mech. **62**, 1 (1996).
[21]H. I. Andersson, J. B. Aarseth, and B. S. Dandapat, "Heat transfer in a liquid film on an unsteady stretching surface," Int. J. Heat Mass Transfer **43**, 69 (2000).
[22]B. S. Dandapat, B. Santra, and H. I. Andersson, "Thermocapillarity in a liquid film on an unsteady stretching surface," Int. J. Heat Mass Transfer **46**, 3009 (2003).
[23]C. H. Chen, "Heat transfer in a power-law fluid film over a unsteady stretching sheet," Heat Mass Transfer **39**, 791 (2003).
[24]M. Van Dyke, *Perturbation Methods in Fluid Mechanics* (Academic, New York, 1964).
[25]A. G. Emslie, F. J. Bonner, and L. G. Peck, "Flow of a viscous liquid on a rotating disk," J. Appl. Phys. **29**, 858 (1959).
[26]B. S. Dandapat, P. Daripa, and P. C. Ray, "Asymptotic study of film thinning process on a spinning annular disk," J. Appl. Phys. **94**, 4144 (2003).